4
EXPERIMENTATION

This chapter presents information about the materials, welding processes, and characterization techniques used in this study. The section on materials in this chapter, discusses the chemical composition of coating constituent minerals, base metals to be welded, and filler metals used for fabricating the weld joint of interest. A brief discussion has also been dedicated to the extreme vertices methodology which has been used to formulate the basic coating composition and its experimental design matrix. The chapter also mentions and discusses various characterization techniques used for studying physicochemical, thermophysical, surface, and structural properties of formulated coatings. Subsequent discussion about the shielded metal arc (SMA) and gas tungsten arc (GTA) welding processes, along with weld characterization techniques, has also been included in later sections of this chapter.

4.1. MATERIALS

The electrode coating has been formulated using calcite, fluorspar, silica, rutile, and mining waste red ochre (Table 4.1). Base metals super duplex stainless steel 2507 grade and API pipeline steel X70 has been joined using shielded metal arc welding (SMAW) and gas tungsten arc welding (GTAW) processes using austenitic stainless steel 309L and super duplex 2594 filler metals (Table 4.2).

Table 4.1: Chemical composition and melting point of coating's mineral constituents (wt. %)

Minerals	Source of	Chemical Composition							Melting Point (°C)
		Calcium	Titanium	Aluminum	Silicon	Sulphur	Magnesium	Iron	
Calcite	CaO	81.55	-	4.91	2.95	-	9.75	0.84	1340
Fluorspar	CaF_2	92.97	-	4.97	1.65	-	-	0.41	1418
Silica	SiO_2	0.56	-	2.82	96.16	0.29	-	0.17	1710
Rutile	TiO_2	-	87.76	5.94	4.33	0.29	-	1.58	1843

Table 4.2: Chemical composition of base and filler metals (wt. %)

Material	Type	Chemical Composition							
		Cr	Ni	Mo	Si	C	N	Mn	Fe
Super duplex 2507	Base Metal	26.2	6.77	3.94	0.48	0.03	0.23	0.82	61.53
API X70		0.006	0.31	0.001	0.32	0.06	-	1.64	97.66
E309L	Filler Metal	23.2	13.4	0.10	0.56	0.02	-	1.92	60.80
E2594		25.6	9.82	3.92	0.34	0.01	0.21	0.53	59.57

The coefficient of thermal expansion for the base and filler metals is summarized in Table 4.3.

Table 4.3: Coefficient of thermal expansion for base and filler metals [Mat. Exp. Coefficients, 2002]

S.No.	Material	Material Type	Thermal expansion coefficient (length/length/°C)
1	Super duplex stainless steel 2507	Base	12.9
2	API X70 pipeline steel	Base	15.3
3	ASS 309L	Filler	14.9
4	Super duplex stainless steel 2594	Filler	12.9

4.2. DESIGN OF EXPERIMENT & FORMULATION OF SMAW ELECTRODE COATING

The basic coating composition for SMAW electrodes was formulated using the extreme vertices design approach as represented in equation 4.1 and equation 4.2 (Mclean & Anderson, 1966; Cornell, 2002). The method considers k ingredients with known lower and upper limits.

$0 \leq \alpha_i \leq Xi \leq \beta_i \leq 100$ (4.1)

$\sum_{i=1}^{n} Xi = 100$ (4.2)

Here, in the above equations, Xi represents the individual constituent in the coating composition, where α_i and βi are the upper and lower limits on that individual constituent. Each coating composition of 'k' constituents can be formulated as a design space that is defined by (k-1) dimensional simplex. For a three constituent mixture system (k=3), the design space is reduced to a two-dimensional simplex, whereas for a four constituent system (k=4), the design space is a tetrahedron (Figure 4.1).

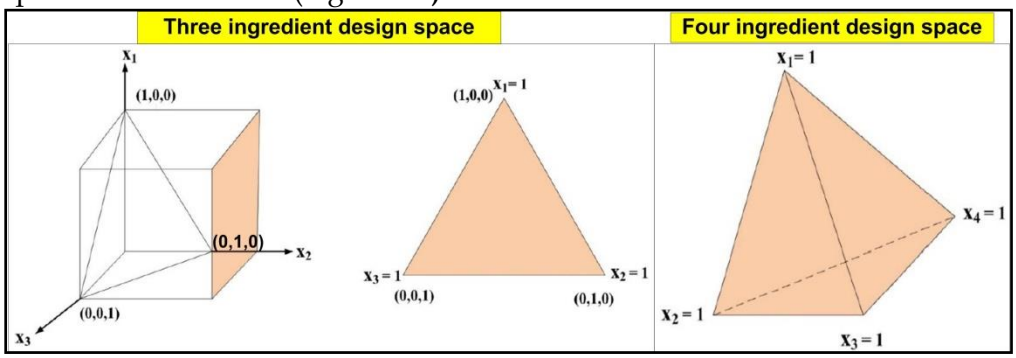

Figure 4.1: Design space for 'k' ingredients

Various design points are specified over the design space as per above mentioned equations 4.1. The points represent different key geometrical locations of three-dimensional space, including overall centroid, vertices, the center of edges, the center of faces, plain center, etc. The proportion of one ingredient is left blank. This procedure produces a total of (2k-1) points. The same process is repeated for all the ingredients by keeping the proportions of one ingredient blank in the list. It will generate a complete list of [k(2k-1)] possible combinations. The proportions of the left-out ingredients in the list are specified in a manner satisfying their lower and upper bound limits and the condition that the sum of all elements must be 100% or unity. In this way, the vertices of the polyhedron are obtained. In the next step, the centroids of the various two-dimensional faces are found by grouping the polyhedron's vertices. The overall centroid of the polyhedron is obtained by averaging all the vertices of the polyhedron. These design points comprise the complete design matrix for experimentation. The observations of output responses are received from which the estimates of the input parameter in the standard mixture design regression models can be calculated. A second-order regression model

represents the output response characteristic of a mixture with 'k' ingredients (equation 4.3**)** **[**Deringer and Suich, 1980].

$$Y = b_0 + \sum_{i=1}^{k} b_i x_i + \sum_{i=1}^{k} \sum_{j=i}^{k} b_{ij} x_i x_j \quad (4.3)$$

Here, b_i and b_{ij} are the least square model regression coefficients; $b_i x_i$ and $b_{ij} x_i x_j$ are the terms denoting individual and interaction of different coating constituents, respectively. The composition in terms of constituents was fixed using the composite melting point approach, which states that for the SMAW electrode, the melting point of electrode coating should be lower than the core filler wire and base metals to be welded. Two ternary phase diagrams (CaO-CaF_2-SiO_2 and CaO-SiO_2-TiO_2) were used to decide the upper and lower limit of constituent minerals (Figure 4.2**)**. An attempt was made to formulate basic type electrode coatings with high basicity index, which would minimize the oxygen and hydrogen level of welds to produce fabricated joints with enhanced structural integrity. The melting point of base metals and core wire lies around 1500°C, hence, a region near 1100-1300°C was chosen as the region of our interest in the two ternary phase diagrams. The maximum combined presence of the four constituents was fixed at 90%, in which a constant amount of red ochre (5% by weight) was further added. The remaining 5% was fixed for the addition of a potassium silicate binder. Table 4.4 and equation 4.4 below summarizes the composition of coating formulated in this study.

Table 4.4: Formulated coating composition (wt. %)

Constituent	Lower Limit	Upper Limit
CaO	25	35
CaF_2	15	25
SiO_2	5	10
TiO_2	20	30
Red Ochre	5 % by weight constant	

$$\sum_{i=1}^{4} x_I = 90 \quad (4.4)$$

Based on the approach mentioned above and constraints, the design matrix of coating formulation was finalized and is summarized in Table 4.5 along with the design space diagram in Figure 4.3.

Table 4.5: Electrode coating compositions

Coating	CaO	CaF_2	TiO_2	SiO_2	Red Ochre	Basicity Index (B.I)
1	30.00	25.00	25.00	10.00	5.00	2.44
2	35.00	20.00	25.00	10.00	5.00	2.44
3	35.00	25.00	20.00	10.00	5.00	3.00
4	32.00	25.00	27.50	5.00	5.00	3.06
5	31.50	21.25	30.00	7.50	5.00	2.66
6	25.00	25.00	30.00	10.00	5.00	2.00
7	32.50	22.50	27.50	7.50	5.00	2.58
8	35.00	17.50	30.00	7.50	5.00	2.33
9	35.00	25.00	25.00	5.00	5.00	3.42
10	35.00	21.25	26.25	7.50	5.00	2.72
11	33.33	23.33	28.33	5.00	5.00	2.95
12	30.00	25.00	30.00	5.00	5.00	2.75
13	31.66	21.66	26.66	10.00	5.00	2.28
14	31.25	25.00	26.25	7.50	5.00	2.72
15	35.00	20.00	30.00	5.00	5.00	2.75
16	35.00	15.00	30.00	10.00	5.00	2.00
17	32.50	22.50	30.00	5.00	5.00	2.75
18	30.00	20.00	30.00	10.00	5.00	2.00
19	35.00	22.50	27.50	5.00	5.00	3.06
20	27.50	25.00	30.00	7.50	5.00	2.33
21	35.00	25.00	22.50	7.50	5.00	3.20

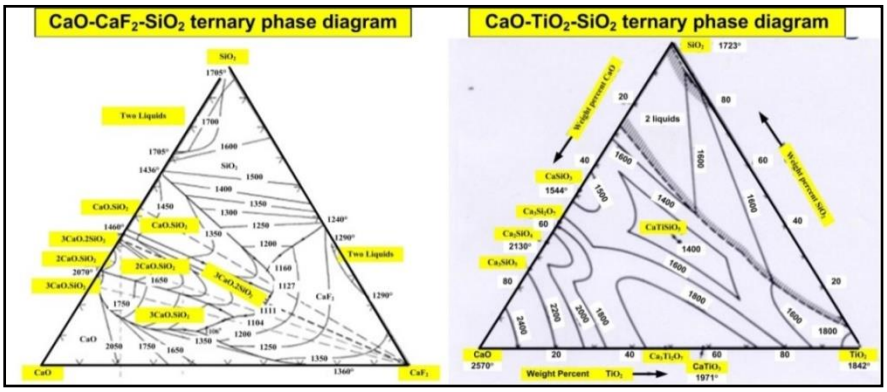

Figure 4.2: Ternary phase diagram (Temperature in °C)

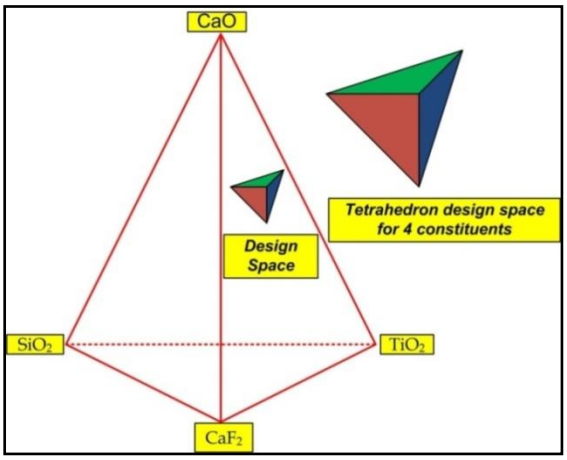

Figure 4.3: Design space diagram

4.3. DEVELOPMENT OF SMAW COATED ELECTRODES

The individual constituents were weighed as per the design matrix and mixed together. The powder mixture was properly blended followed by the addition of 10mL potassium silicate binder before adding into the muller. The mixture was left in muller for 30 minutes to obtain a wet mix. This wet mixture of coating composition was then extruded on the core filler wire austenitic 309L of diameter 3.2mm in a laboratory-scale electrode extruder. The extruded electrodes were air-dried for 24 hours, followed by 90 minutes of oven baking at a temperature of 360°C. A schematic representation of electrode extrusion is shown in Figure 4.4.

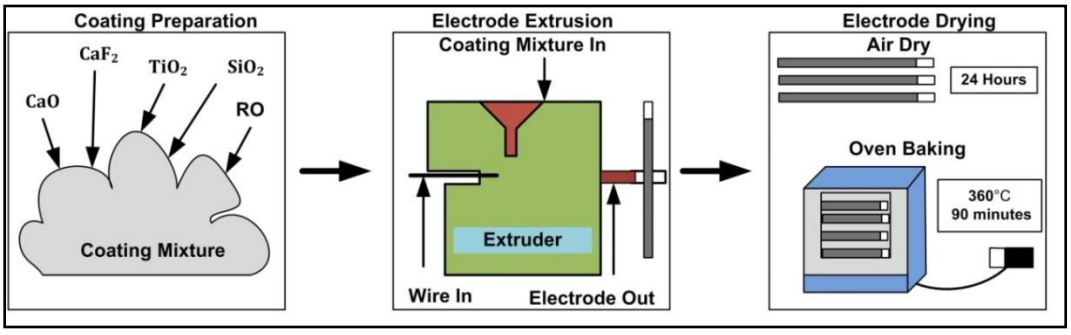

Figure 4.4: Electrode extrusion process [RO: Red Ochre]

4.4. CHARACTERIZATION OF ELECTRODE COATING

The coated electrode prepared as per the method described in section 4.3 was then hammered to break and separate the coating from the core wire. The broken coating was crushed to prepare its uniform powder for further characterization. The obtained electrode coating compositions were characterized for physicochemical, thermophysical, structural, and wettability properties.

This section discusses the various instruments and methodology adopted for characterizing the coating.

4.4.1. PHYSICOCHEMICAL AND THERMOPHYSICAL PROPERTIES

The density of coating was estimated at room temperature using the tap density method. The crushed powder for each coating composition was filled up to 10 mL mark in a laboratory test tube. This powder was then weighed in an electronic weighing balance to obtain the amount of powder that would occupy 10 mL space in the test tube. Further, using equation 4.5, the density for each composition was estimated.

$$\text{Density } (\rho) = \frac{Mass\ in\ grams\ (m)}{Volume\ \ in\ mL\ (V)} \quad (4.5)$$

The thermal stability and enthalpy of fusion for the electrode coatings were calculated in a Simultaneous Thermal Analyzer (STA) using Thermo Gravimetric Analysis (TGA). In this experimentation, around 10-12 grams of coating powder was heated in a controlled environment from an initial temperature of 30°C to 890°C at a constant heating rate of 20°C/min. The software interphase of this instrument measures the initial and final weight of the specimen, thereby giving the %loss in weight as an indicator of thermal stability. Moreover, the area under the heat flow versus temperature curve gives the enthalpy of fusion, indicating the amount of heat released by the coating upon being subjected to the test as mentioned above. The thermal properties of conductivity, diffusivity, and specific heat were obtained using the hot disc measuring apparatus employing a Kapton sensor. The sensor is in touch with and surrounded by crushed coating powder. The heat flow through the sensor then gives an estimate of the thermal properties of the powder specimen.

4.4.2. STRUCTURAL ANALYSIS

X-ray diffraction (XRD) and Fourier transform infrared spectrometer (FTIR) was used for conducting the structural analysis of electrode coatings. Different phases present in coating composition were estimated using XRD, scanning in the range of 10° to 90° at a scan rate of 1°/min. FTIR scan in the wavelength range 400-4000 cm^{-1} was performed to identify different bonds present in the coating mixture.

4.4.3. WETTABILITY PROPERTIES

Wettability properties define how electrode coating will cover the weld bead after melting. The cylindrical pellets of height 13 mm and diameter of cross-section 10 mm were prepared and then exposed to a high temperature of 1150°C for 120 seconds to initiate the partial melting. The pellets were placed upon the super duplex stainless steel strip of dimension 50x50x2 mm melted in a high-temperature muffle furnace. The super duplex strips in the thickness of 6 mm were polished up to 600 grade SiC emery papers to give uniform melting surface to coating of all formulated compositions. The melting surface was cleaned using acetone to remove any dirt, oxide or unwanted particels. The pellet was taken out from the furnace after the exposure time of 120 seconds, and its images were taken using high-resolution photography from the top and side view. These images were then analyzed on Image J software to find the contact angle and spread area. The measured contact angle was then used to find the interfacial tension and work of adhesion. Young's equation (equation 4.6) was further used to correlate the surface and interfacial tension at different boundaries of molten liquid in equilibrium conditions.

$$\gamma_{SL} = \gamma_{SG} + \gamma_{LG} \cos\theta \quad (4.6)$$

Where γ_{SL} and γ_{SG} are the interfacial tension in the units of mN/m at the solid-liquid and solid-gas interphase respectively, θ in degrees is the contact angle, whereas γ_{LG} represents the surface tension of molten powder pellet in equilibrium condition. Figure 4.5 below gives a pictorial representation of wettability parameters. Boni's empirical equation is used to estimate the surface tension of molten pellet (equation 4.7**)** (Kim et al., 2015).

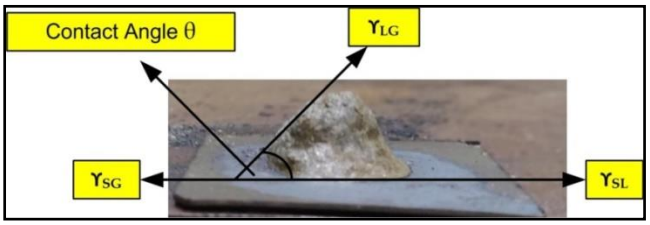

Figure 4.5: Wettability parameters

$$\gamma_{LG} = x_1f_1 + x_2f_2 + x_3f_3 + \ldots\ldots\ldots + x_nf_n \quad (4.7)$$

Where x_n is the percentage mole fraction of the component, whereas f_n is its surface tension factor. The surface tension factor values as a function of exposure temperature for coating constituent minerals was found using available literature (Kingery et al., 1953; Shigeta et al., 1989; Yanhui et al., 2014; Kim et al., 2015) (Table 4.6). Adhesion energy, often termed as Work of Adhesion (W_a) is another important parameter that measures the amount of energy required to remove the molten metal from the contacting surface. It is the amount of force required to cross over the threshold of interphase energy between the molten liquid and solid substrate. Adhesion energy varies indirectly with the contact angle. Work of adhesion (W_a) can be calculated using Dupre –Young equation (equation 4.8) (Joshi et al., 2017).

Table 4.6: Surface tension factor of constituent minerals

S. No	Mineral	Surface Tension Factor (f_n)
1	CaO	791 - 0.0935 T
2	CaF_2	407.75 – 0.07 T
3	TiO_2	1384.3 – 0.6254 T
4	SiO_2	243.2 + 0.031 T

$$W_a = \gamma_{LG}(1 + \cos\theta) \quad (4.8)$$

4.5. MULTI PASS BEAD ON PLATE EXPERIMENT

The 21 electrode coatings formulated as per the design matrix and extruded on austenitic 309L filler wire were used to make multi pass beads on 6 mm thick super duplex stainless steel 2507 grade steel. The 100 mm x 25 mm bead on plate were deposited using shielded metal arc welding (SMAW) set up at a constant current of 90A and 25V voltage. The multi pass bead on plate welding parameters was chosen based on several pre-trails which included altering the current. The pre-trial current values and corresponding qualitative observations have been summarized in Table 4.7 below.

Table 4.7: Qualitative observation of trail parameter

Current (A)	Arc stability	Slag detachability	Bead appearance
80	Fair	Fair	Poor
85	Fair	Fair	Fair
90	Good	Good	Good

The deposited weld beads were then subjected to qualitative and quantitative characterization. The qualitative characterization was done by observing the slag detachability, ease of arc

initiation, continuity, and bead profile. Whereas the quantitative evaluation includes the microhardness and weld bead chemistry obtained using an atomic absorption spectrometer. Analysing the results of these characterizations, two coating compositions were chosen from the set of twenty-one formulations to fabricate a dissimilar shielded metal arc weld between super duplex stainless 2507 and API X70 grade pipeline steel.

4.6. REGRESSION ANALYSIS

The regression models for laboratory-developed electrode coating mixture's physicochemical, thermophysical, wettability properties, and weld chemistry were developed using mixture design approach. ANOVA technique was applied, and each output was analysed. The developed models were also optimized for multiple responses. An optimized set of solution from the design space was obtained with a desirable target set for each property of interest. Regression models were confirmed against an acceptable confidence level of 95%, and the influence of flux coating constituents and their binary, tertiary interactions on output properties were established.

4.7. FABRICATION OF WELDS

The dissimilar weld between super duplex stainless 2507 and API, X70 grade pipeline steel, has been fabricated using two different processes; shielded metal arc welding (SMAW) and gas tungsten arc welding (GTAW). Coupons of dimensions 250mm* 70 mm*15 mm were machined from both the materials, and edges were machined to an angle of 30° each with a root face of 2mm and root gap of 3mm. Figure 4.6 below represents the weld coupon geometry. This section further discusses the process and the parameters of welding used in this study.

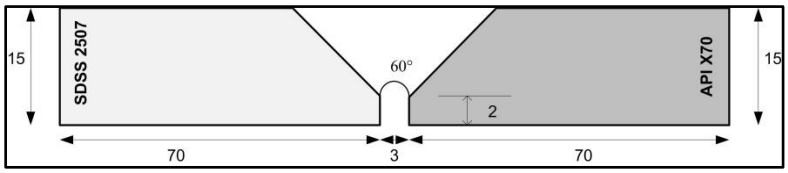

Figure 4.6: Weld joint design (all dimensions in mm)

4.7.1. SHIELDED METAL ARC WELDING (SMAW)

The shielded metal arc welds were fabricated at a current of 110A and welding speed of 2mm/sec maintaining the average heat input of 0.275kJ/mm. The detailed information about parameters for each weld pass is given in section 5.5.1 of chapter 5. Four C-clamps were used for holding the coupons in place to avoid bending in the weld. The root pass was made with austenitic 309L filler wire (2.1mm diameter) using the GTAW process. A total of three SMA welds were fabricated, two from the laboratory-developed coatings and one from the commercial electrode.

4.7.2. GAS TUNGSTEN ARC WELDING (GTAW)

The dissimilar GTA weld between the above-mentioned materials was fabricated using two candidate fillers; (i) austenitic 309L and (ii) super duplex filler 2594 grade. Multi pass weld was fabricated by filling the 60° single V groove geometry. The current and voltage in the process were kept as 170A and 15V, whereas pure argon (99.999%) gas was purged at a constant flow rate of 15 L/min. The heat input was 0.51kJ/mm calculated using HI= ηVI/S, where V and I are the voltage and current, S is the welding speed in mm/min which was kept approximately 3mm/sec, and η is the efficiency of the process, which is usually taken 0.65 for GTAW process (TWI). The wire feed rate was kept 8cm/min. A non-consumable tungsten electrode AWS EWTH-2 (98%W + 2%Th) was used along with the above-mentioned grades of the filler wires in

the wire diameter of 2.4mm. The electrode tip to work distance was maintained at 3mm for the entire pass length.

4.8. METALLURGICAL AND MECHANICAL CHARACTERIZATION

The base metals, deposited multi-pass bead on the plate, and fabricated welds were subjected to several metallurgical and mechanical characterizations. Different experimental techniques were used to characterize them for various performance properties to ascertain the structural integrity of the component employing them. This section further discusses in detail the multiple characterizations carried out in this study.

4.8.1. METALLURGICAL CHARACTERIZATION

The base and weld metals were examined for their microstructure and elemental composition using an optical and scanning electron microscope (SEM) equipped with an energy dispersion spectroscope (EDS). The microscopy specimens were polished on emery papers from SiC papers with grit size from 80 to 1200 followed by successive polishing against diamond suspension of 3 μm, 1μm and 0.25μm. The mirror-polished specimens were then etched with etchants, as mentioned in Table 4.8. The etched specimens were examined for microstructures. Atomic absorption spectrometry, dilution calculations and EDS analysis was used to find the elemental composition in the different zones. The microscopy specimens were further polished in colloidal silica solution against the velvet cloth for EBSD characterization. EBSD was carried out to obtain the information about grain angle boundaries, misorientation, and grain size in terms of ferret diameter (μm). The phase estimation of different phases in the weld and Scheil's solidification calculation for each weld was done using ThermoCalc software. The weld specimen were also subjected to electron probe micro analyzer (EPMA) to quantify the elemental partitioning occurring at the interface of X70 heat affected zone and weld fusion zone boundary. XRD measurement of base metals and weld fusion zone was carried out in the diffraction angle range of 20° to 100° followed by the reitveld refinement to perform structural verification in terms of phases, peak identification, and phase ratio estimation.

Table 4.8: Etchants used for microstructure investigations

S.No	Material	Region	Etchant	Chemical composition
1	Super duplex stainless steel 2507 grade	Base metal	Villela reagent	1g picric acid + 5ml HCl + 100 ml ethanol
2	API X70 grade steel	Base metal	2% Nital solution	10ml nitric acid + 100ml ethanoL
3	Austenitic stainless 309L grade	Weld fusion zone	10% oxalic acid	3.15g oxalic acid + 250ml distilled water
4	Super duplex stainless steel 2594 grade	Weld fusion zone	Villela reagent	1g picric acid + 5ml HCl + 100 ml ethanol

4.8.2. MECHANICAL CHARACTERIZATION

Specimens were extracted from welds to characterize it for mechanical properties of tensile strength, impact energy, microhardness, wear behavior, and corrosion resistance. Table 4.9 below represents the detail of various tests performed for mechanical characterization in this work. The tensile, impact, and hardness specimen were extracted in across the weld orientation. Whereas the tribology specimen in the shape of pin was extracted from into the weld orientation comprising of all weld metal. The corrosion specimens were extracted from the weld fusion and heat affected zones on both the sides. The corrosion test was performed in the aqueous

environment of 3.5% NaCl solution at a scan rate of 0.167 mV/s. The three electrode system uses, Ag/AgCl electrode as reference, specimen as working and graphite rod as counter electrode. The potential range was kept -0.25V to +0.25V versus the specimen's open circuit voltage.

Table 4.9: Mechanical characterization of welds

S. No.	Mechanical Property	Instrument Used	Standard
1	Tensile strength	Universal Testing Machine	ASTM A370
2	Impact strength	Charpy impact tester	ASTM E23-18
3	Hardness	Microhardness tester	ASTM E384
4	Wear resistance	Pin on disc tester	ASTM G99-17
5	Corrosion resistance	Electrochemical workstation	ASTM G5-94

A schematic representation of characterization specimens is shown in Figure 4.7.

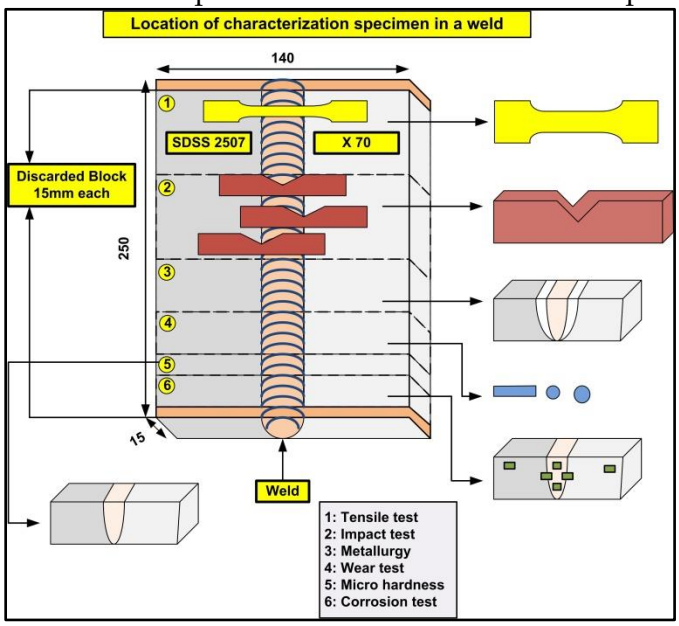

Figure 4.7: Schematic representation of characterization specimens

Multiple specimens of each type were tested for mechanical properties. From the obtained results, the highest and lowest values were discarded, and the mean value of remaining observations has been reported in this study. This method was applied for all the specimen types (base metal and welds) to ensure repeatability and uniform comparison.

Summary of Chapter 4:

Experimental techniques in this work range from characterizing mineral powders to base metals followed by comprehensive investigations on fabricated welds. This chapter presented the detailed description of various experimental methods adopted in this work. Chemical composition of base metals, coating's mineral constituents along with testing parameters for each experimental characterization has been provided. ASTM standards followed for each test has been mentioned. Brief information about welding parameters has been given which will be further discussed in detail in Chapter 5. The chapter also serves as a primary reading for Chapter 5, which will discuss in detail the results obtained from these experiments and subsequent inferences drawn from them.